Power Electronic Systems
Laboratory

Proceedings of the 41th Annual Conference of the IEEE Industrial Electronics Society (IECON 2015), Yokohama, Japan, November 9-12, 2015

Impact of Transcutaneous Energy Transfer on the Electric Field and Specific Absorption Rate in the Human Tissue

O. Knecht,
J. W. Kolar

Eidgenössische Technische Hochschule Zürich
Swiss Federal Institute of Technology Zurich

IECON2015-Yokohama
November 9-12, 2015

Impact of Transcutaneous Energy Transfer on the Electric Field and Specific Absorption Rate in the Human Tissue

O. Knecht, and J. W. Kolar
Power Electronic Systems Laboratory, ETH Zürich, Switzerland, Email: knecht@lem.ee.ethz.ch

***Abstract*—Inductive power transfer technology has proven to be a promising solution for powering implantable heart pumps such as left ventricular assist devices, eliminating the need for a percutaneous driveline and reducing the risk of severe infections significantly. However, the required high power transfer capability of a Transcutaneous Energy Transfer (TET) system raises questions about human safety regarding the exposure to electric and magnetic fields. The focus of this paper is on the internal electric fields and the Specific Absorption Rate (SAR) caused by a prototype TET system designed to transfer 30 W across the skin at 800 kHz and 35 V output voltage. Numerical simulations show that the internal electric field and the SAR can locally attain high values within the fat tissue due to the large voltage potential at the implanted coil terminals. It is further shown that the parasitic capacitances of the energy transmission coils and the power electronic circuit of the implant can cause common-mode voltages at the energy receiving coil terminals, which increase the internal electric field strength additionally. Hence, the power electronic circuit and the grounding scheme of the system need to be adapted in order to eliminate common-mode voltages. As an additional countermeasure, an electric shielding based on carbon conductive compounds is presented in this paper, which is able to reduce the maximum internal electric field strength from 224 V/m to 77 V/m and the maximum SAR and from 1.21 W/kg to 0.25 W/kg with only 1 % of additional power loss.**

***Index Terms*—Inductive power transfer (IPT), transcutaneous energy transfer (TET), specific absorption rate (SAR), electric shielding, common-mode**

I. Introduction

As society in the industrial nations is growing older, the number of people with advanced heart failure is increasing. Due to the lack of availability of suitable donor organs, extensive research in the field of Mechanical Circulatory Support Systems (MCSS), such as Left Ventricular Assist Devices (LVADs), was carried out to provide transitional treatment as a bridge to transplantation. Since its origin in 1960 [1], LVAD technology underwent significant innovation such that the patients live with an LVAD for months or even years [2]. Nevertheless, device related failure and infections are still a dominant factor and can complicate the assist device support substantially [3]. Due to the continuous high power consumption of an LVAD, a driveline is used today to supply the electrical power to the implanted mechanical blood pump. This permanent damage of the skin can lead to severe infections and reduces the quality of life for the patient [4].

In response to this drawback, Wireless Power Transfer (WPT) technology evolved to be a promising solution to replace the driveline and to supply energy to the implant without the need for direct galvanic contact [5]. In order to allow for an untethered operation of the LVAD, a backup battery storage is included in a fully implantable MCSS. Therefore, including the recharging of the backup battery, the maximum power consumption of the implanted device is in a range of 25-30 W. Hence, the high power transfer capability requirement imposes significant challenges in the design and optimization of a Transcutaneous Energy Transfer (TET) system and gives raise to major concerns regarding the potential safety risks.

There are mainly three effects that could constitute a potential risk to the human organism. First, the power losses in the energy receiver coil can be significant and are causing heating of the surrounding tissue, which can lead to permanent tissue damage [6], [7]. Second, the magnetic field in the TET system induces eddy currents in the tissue. These currents can evoke stimulation of nerve cells and muscle tissue, and cause additional heating. Third, depending on the power electronic converter topology used for the operation of the TET system, the electric fields due to the voltage potential at the power transfer coils can significantly contribute to the energy absorbed in the tissue and can excite electrically sensitive tissue.

In literature, the impact of magnetic fields on the human body is widely studied for WPT systems which are operated outside of the human body [8]–[11], as well as for low power medical implants [12] and for a few TET systems powering an LVAD [13], [14]. However, the influence of electric fields, which are particularly important for high power TET systems, is often neglected.

Therefore, the main topics of this paper are the investigation of the effect of the electric fields in the vicinity of the wireless power receiver and its impact on the exposure of the human tissue. The results are demonstrated with a recently developed TET system prototype [15] and the exposure of the tissue to the electromagnetic fields is evaluated for compliance with established safety guidelines such as the FCC 96-326 [16], ANSI/IEEE C95.1-2005 [17], ICNIRP 1998 [18] and ICNIRP 2010 [19]. In addition, the impact of common-mode (CM) voltage in the TET system on the electric field is discussed. Finally, guidelines are provided on how to design the TET system such that the internal electric field and the absorbed energy are minimized.

II. Exposure Mechanisms and Standards

In order to evaluate the human exposure to time-varying electromagnetic fields (EMF) of a WPT system in close proximity or in direct contact with human tissue, it is important to understand how the electric and magnetic fields interact with the tissue. Since the human body has the permeability of air, the magnetic field of a WPT system is barely disturbed by the tissue. However, biological tissue has a frequency dependent conductivity and permittivity and behaves like a lossy dielectric. Hence, eddy currents can be induced by time-varying magnetic fields and dielectric losses as well as conduction losses occur due to induced and applied electric fields. Depending on the operating frequency, the dominant mechanism of interaction changes. The frequency range from 100 kHz up to 10 MHz, which is the usual operating frequency range of most TET prototype systems, represents a transitional stage where above 100 kHz the heating of the tissue due to radio frequency energy absorption becomes relevant and below 10 MHz, the internal electric fields and the induced currents can excite electrically sensitive tissue [18], [19]. Consequently, EMF exposure can be quantified in the specified frequency range in terms of the internal electric field strength, induced current density and Specific Absorption Rate (SAR), which is a measure of the time-average of the absorbed power per unit mass of tissue, specified as watts per kilogram and is given as

$$\mathrm{SAR} = \frac{\sigma |\underline{E}|^2}{\rho} \,, \tag{1}$$

978-1-4799-1762-4/15/$31.00 ©2015 IEEE

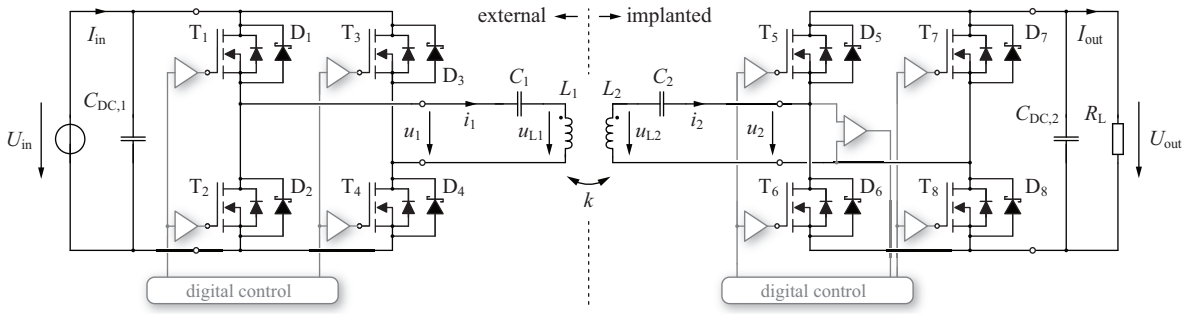

Figure 1: Schematic drawing of the prototype TET system described in [15].

Guideline	Frequency	RMS Current Density $\left(\frac{\mathrm{mA}}{\mathrm{m}^2}\right)$		RMS Electric Field Strength $\left(\frac{\mathrm{V}}{\mathrm{m}}\right)$	
		occupational	general pubic	occupational	general public
ICNIRP 1998 [18], 2010 [19]	100 kHz - 10 MHz	$f_{\mathrm{Hz}}/100$	$f_{\mathrm{Hz}}/500$	$2.7 \cdot 10^{-4} \cdot f_{\mathrm{Hz}}$	$1.35 \cdot 10^{-4} \cdot f_{\mathrm{Hz}}$
IEEE 2005 [17]	3.35 kHz - 5 MHz	-	-	$6.27 \cdot 10^{-4} \cdot f_{\mathrm{Hz}}$	$2.09 \cdot 10^{-4} \cdot f_{\mathrm{Hz}}$

Table I: Basic restrictions on the induced current density and the internal electric field strength in the trunk of the human body.

Guideline	Avg. Mass	SAR $\left(\frac{\mathrm{W}}{\mathrm{kg}}\right)$	
	(g)	occup.	gen. public
ICNIRP 1998 [18]	10	10	2
IEEE 2005 [17]	10	10	2
FCC 1996 [16]	1	8	1.6

Table II: Basic restrictions on the local specific absorption rate (SAR) evaluated for the specified averaging mass of tissue, for occupational and general public exposure.

where σ is the electrical conductivity and ρ is the density of the tissue material. The SAR is proportional to the square of the RMS electric field strength $\underline{E}$ and is usually averaged over a tissue volume with a mass of 1 g or 10 g for local EMF exposure assessment.

The most widely discussed guidelines for limiting exposure to EMF is proposed by the International Commission on Non-Ionizing Radiation Protection (ICNIRP) [18], [19] which provides exposure limits in terms of basic restrictions on SAR, electric field strength and induced current density, that are based directly on established health effects. In the latest guideline published by the ICNIRP (2010), the induced current density has been replaced by the internal electric field strength as a limiting quantity concerning the stimulation of nerve cells and electrically sensitive tissue up to 10 MHz [19]. Besides the ICNIRP guidelines, different guidelines such as the IEEE C95.1-2005 [17] and the FCC 96-326 [16] apply depending on the country of interest. **Tab. I** and **Tab. II** summarize the basic restrictions on SAR, internal electric field strength and induced current density for a frequency range of 100 kHz to 10 MHz. In the guidelines, there is an additional distinction between occupational and general public exposure, where the occupationally exposed population is trained to be aware of the potential risks. In contrast, the general public population, which comprises individuals of all ages and health status, is protected by more stringent safety limits [18].

In the case of a TET system, where the energy receiver circuit is implanted into the subcutaneous tissue, local effects of the EMF exposure are highly important. Therefore, for the exposure assessment presented in this paper, the peak values were considered in the safety analysis and not the averaged values proposed by the safety guidelines. In addition, the most restrictive limits are applied for both, the internal electric field and SAR in order to provide a conservative estimation of the EMF exposure.

In order to understand the mechanisms in a TET system, that can contribute to the EMF exposure, the converter topology and the operation principle of a TET system is reviewed in the next section.

III. TET System Operation

The basic circuit of the prototype TET system presented in [15] is shown in **Fig. 1**. A primary and secondary side coil are used to form a loosely coupled transformer which allows to transfer energy through the skin. A full-bridge inverter supplies the transmitter coil which is placed close to the surface of the skin above the implanted receiver coil. On the secondary side a synchronous rectifier is used to convert the induced AC voltage into a DC output voltage. Due to the large coil separation distance and the limited coil diameter, the magnetic flux generated by the primary coil is only partially linked to the secondary side coil. This weak coupling limits the power transfer capability and the power transmission efficiency of the system. In order to enhance the system performance, the TET coils are operated in a resonant converter structure using resonant capacitors on the primary and secondary side in order to compensate for the large stray inductances.

For low power medical implants, the parallel compensation method is often used, where the secondary side resonant capacitor is placed in parallel to the energy receiver coil. However, this method has the disadvantage that the additional reactive current in the resonant tank causes power losses in the receiver coil even at light load conditions. In contrast, in a series-series compensated topology as it is shown in **Fig. 1**, only the load current is present in the secondary side resonant tank which reduces the secondary side power losses in partial load operation significantly. Therefore it was decided to use a series-series compensation topology for the prototype TET system. The specifications of the TET coils and the operating conditions used for the EMF exposure analysis are summarized in **Tab. IV**.

The main disadvantage of the series-series compensation topology is the high voltage potential occurring at the receiver coil terminals at high load conditions. As a result, an electric field with high magnitude is present in close proximity to the receiver coil and can substantially contribute to the EMF exposure. This effect will be analyzed in the following sections.

Model Material ($f_0 = 800$ kHz)		Skin (dry)	Skin (wet)	Fat	Muscle	Cortical Bone	Bone Marrow (red)	Lung (inflated)
Rel. Permittivity		1019.1	2271.4	52.4	2336.9	155.3	102.0	818.3
El. Conductivity	$\left(\frac{\mathrm{S}}{\mathrm{m}}\right)$	0.0093	0.2070	0.0439	0.4852	0.0235	0.1039	0.1311
Density	$\left(\frac{\mathrm{kg}}{\mathrm{m}^3}\right)$	1109.0	1109.0	911.0	1090.4	1908.0	1028.5	394.0
Layer Thickness	(mm)	0.2	1.2	13.6	15.0	1.0	3.0	70.0

Table III: Human tissue properties [20], [21] evaluated for the prototype TET system operating frequency of 800 kHz. The last line of the table specifies the thickness of the layer of tissue used in the finite element simulation model.

(a) Energy Transmission Coils	
Inductance L_1, L_2	18.8 µH, 18.4 µH
AC resistance R_{L1}, R_{L2}	210 mΩ, 204 mΩ
Litz wire	300 x 0.04 mm
Number of turns	16
Outer coil radius R_a	35 mm
Inner coil radius R_i	17 mm
(b) Operating Conditions	
Switching frequency f_0	800 kHz
Output voltage U_{out}	35 V
Output power P_{out}	30 W
Coil separation distance d_{c}	15 mm
Coupling factor k	0.35

Table IV: Energy transmission coil specifications and operating conditions of the prototype TET system.

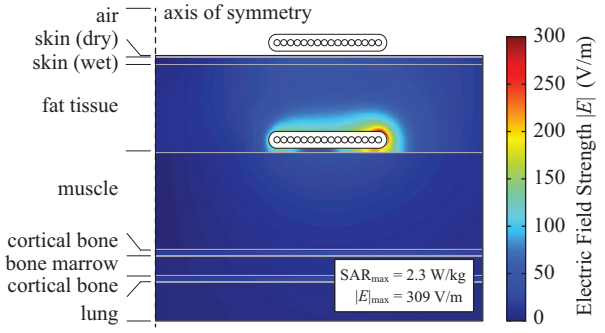

Figure 2: Simulation model geometry and simulation result of the electric field strength in the human tissue for the operating condition of the prototype TET system specified in **Tab. IV(b)** and the converter topology shown in **Fig. 1**

IV. Simulation Model

In order to predict the magnitude of the internal electric field and the energy absorbed in the human tissue, a two dimensional simulation model of the human skin and the subcutaneous tissue was created in a Finite Element Method (FEM) based simulation tool. The model is built rotational symmetric and the prototype TET coils are modelled with each individual turn of the winding, embedded in a silicone insulation layer. The receiver coil is located within the fat tissue directly above the muscle e.g. in the upper chest of the patient. Therefore, the layer structure shown in **Fig. 2** is used for the simulations. The material properties of the human tissues are taken from [20], [21] and are summarized in **Tab. III**. The electrical conductivity and the permittivity of the tissues can be computed for the desired operating frequency by means of a 4-Cole-Cole dispersion model [21], using the equation parameters provided by [20], [21]. For the silicone insulation, an electrical conductivity of $2.5 \cdot 10^{-14}$ S/m and a relative permittivity of 2.8 is used.

The human tissue is exposed to the electromagnetic near-field of the energy transmission coils. Therefore, in order to simplify the problem, a quasistatic approximation of the Maxwell's equations was used, such that the electric and the magnetic field can be calculated separately. This approximation is valid since the considered simulation volume is sufficiently small compared to the wavelength in the considered materials and hence, the electric and magnetic fields are propagated instantaneously within the tissue [9], [22]. Accordingly, the problem is split into an electro-quasistatic and magneto-quasistatic problem. The total electric field and current density in the tissue is then obtained from the superposition of the solutions obtained from the electro- and magneto-quasistatic problems. This approach is valid as long as the material properties are linear with respect to the magnitude of the electric and magnetic field.

As an excitation source for the magneto-quasistatic problem, the current in each coil is specified with a homogeneous current density. For the electro-quasistatic problem, the excitation is defined as voltage potential for each individual turn of the TET coils. With good approximation, the electric potential is distributed linearly across the coil winding and the amplitude of the primary and secondary side coil terminal voltages can be calculated using an equivalent circuit model of the resonant converter as shown in **Section V**.

In order to calculate the electric field in the tissue, the electric potential of the surrounding tissue with respect to the implant must be determined. However, this raises the question on how the implanted electronic circuit is connected to the human body. Due to the capacitive coupling of the energy transmission coils to the surrounding tissue and depending on the grounding scheme of the implanted power electronic circuit, CM currents can flow in the tissue. Hence, a CM voltage can be present at the TET coil terminals with respect to the tissue, which causes an increase of the electric field strength. This effect will be studied in more detail in the next section.

V. Influence of Common-Mode Voltage

In a first step, in order to determine the applicable excitation sources for the electro-quasistatic simulation, a simplified electrical equivalent circuit model of the human skin and subcutaneous tissue is used to predict the magnitude of the CM voltages. Second, the numerical simulation model is used to evaluate the influence of the CM voltage on the EMF exposure. And third, the effect of the grounding scheme of the implanted power electronics is reviewed and *in vitro* measurements using the prototype TET system are provided to validate the theoretical considerations.

A. Electrical Equivalent Circuit Model

In order to analyze the CM current paths, an equivalent circuit of the prototype TET system and the subcutaneous tissue can be created to model the electrical environment for the implanted electronic components as it is shown in **Fig. 3**. Similar to the method of impedances described in [23], the indicated resistors and capacitors which represent the electric impedance of the tissues are calculated in

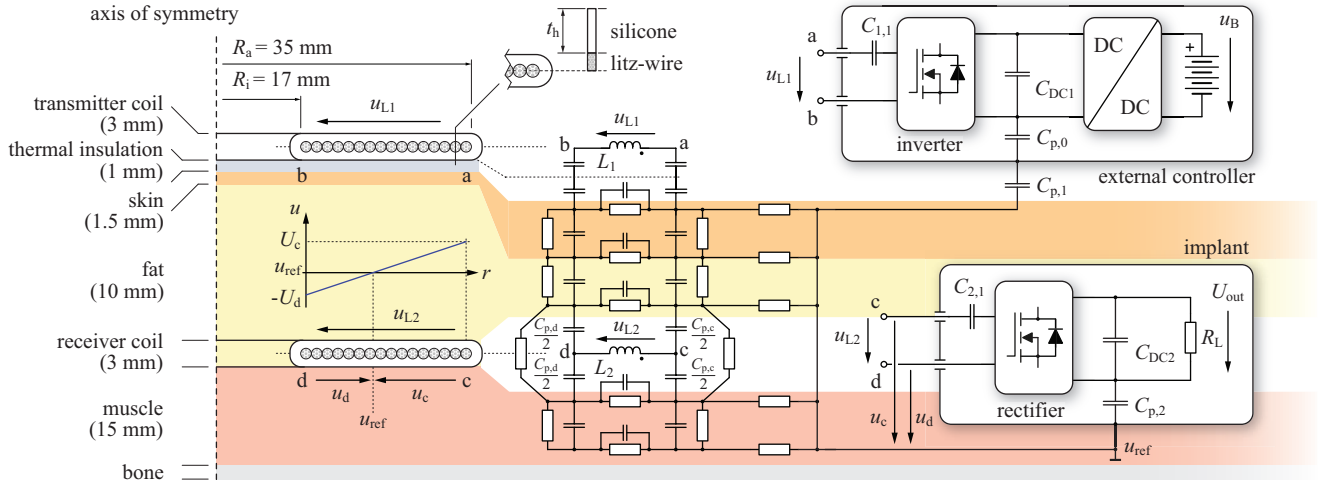

Figure 3: Simplified drawing of the layers of the subcutaneous tissue and the location of the energy transmitter and receiver coil. A simplified equivalent circuit of the tissue is shown, which is used to model the electrical environment in which the receiver coil and the implanted controller are operated.

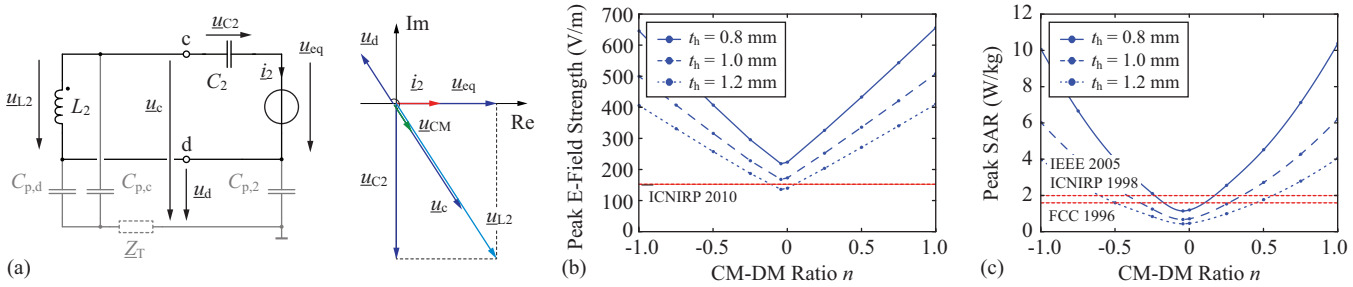

Figure 4: (a) AC equivalent circuit of the energy receiver within the tissue and phasor diagram of the indicated voltages. (b) and (c) show the peak electric field strength and the peak SAR in the tissue as a function of the ratio between the coil common-mode (CM) and differential-mode (DM) voltage with respect to the human body.

this case for a very coarse mesh of sub-volumes. The details of this calculation are omitted here. As the main result, the model showed that the magnitude of the total tissue impedance $|\underline{Z}_T|$ in **Fig. 4(a)** between the TET coils and the implanted controller varies between 250 Ω and 280 Ω, if the controller is located at 200 mm distance from the TET coils.

The parasitic capacitances $C_{p,c}$ and $C_{p,d}$ formed by the implanted coil and the surrounding tissue are calculated to be in a range of 60-85 pF for the prototype TET system and a coil insulation layer thickness of 1 mm. The parasitic capacitance $C_{p,2}$ is highly dependent on the actual design of the implantable controller and the power electronic circuit and values vary between 10 pF and 100 pF. Accordingly, the tissue impedance $\underline{Z}_T$ can be neglected initially, compared to the impedances of the parasitic capacitances at the operating frequency of the prototype TET system. Further it is assumed, that the capacitive coupling $C_{p,1}$ of the external controller to the human body is very small, such that the CM voltage at the transmitter coil terminals with respect to the human body is negligible. Using this approximations, a simplified AC equivalent circuit of the implanted receiver circuit can be created as shown in **Fig. 4(a)** along with the phasor diagram for the general case in which a CM voltage applies at the coil terminals. The phasor diagram shows that the voltages $\underline{u}_c$ and $\underline{u}_d$ are phase-shifted by 180 ° as long as $\underline{Z}_T$ is small. This implies that there is a turn in the receiver coil that has the same voltage potential as the surrounding tissue and that the voltage potential is distributed asymmetrically across the winding with respect to the tissue, such that one coil terminal experiences a higher voltage stress than the other.

In order to describe this asymmetry and its impact on the EMF exposure, the ratio between the amplitudes of the CM voltage $\hat{U}_{CM}$ and the Differential-Mode (DM) voltage $\hat{U}_{DM}$ is defined as

$$n = \frac{2\hat{U}_{CM}}{\hat{U}_{DM}} = \frac{\underline{u}_c + \underline{u}_d}{\underline{u}_c - \underline{u}_d} \approx \frac{C_{p,d} + C_{p,2} - C_{p,c}}{C_{p,d} + C_{p,2} + C_{p,c}} . \quad (2)$$

The CM-CM ratio can be calculated approximatively using the previous assumption that the impedance of the tissue $\underline{Z}_T$ is much smaller than the impedances of the parasitic capacitances $C_{p,c}$, $C_{p,d}$ and $C_{p,2}$. In this case, the ratio depends only on the capacitive voltage divider formed by the parasitic capacitances $C_{p,d}$, $C_{p,d}$ and $C_{p,2}$. Using (2) and the estimated values for the parasitic capacitances, a CM-DM ratio of 0.05 to 0.45 is estimated for the prototype TET system.

B. *Effect of CM Voltage*

Using the results of the previous section, the voltage potentials at the receiver coil can be defined in the electro-quasistatic simulation, which allows to compute the EMF exposure of the surrounding tissue. **Fig. 4(b)-(c)** shows the FEM simulation results of the maximum internal electric field strength and the peak SAR for a variable CM-DM ratio and for a coil insulation layer thickness of 0.8 mm, 1.0 mm and 1.2 mm, respectively, for the operating conditions specified in **Tab. IV(b)**. It was assumed that the differential coil voltage u_{L2} is sinusoidal and has the amplitude of the actual maximum coil terminal voltage which is given by $\hat{U}_{L2} = \hat{U}_{C2} + U_{out}$. It can be seen that the maximum electric field strength rises linearly with increasing CM

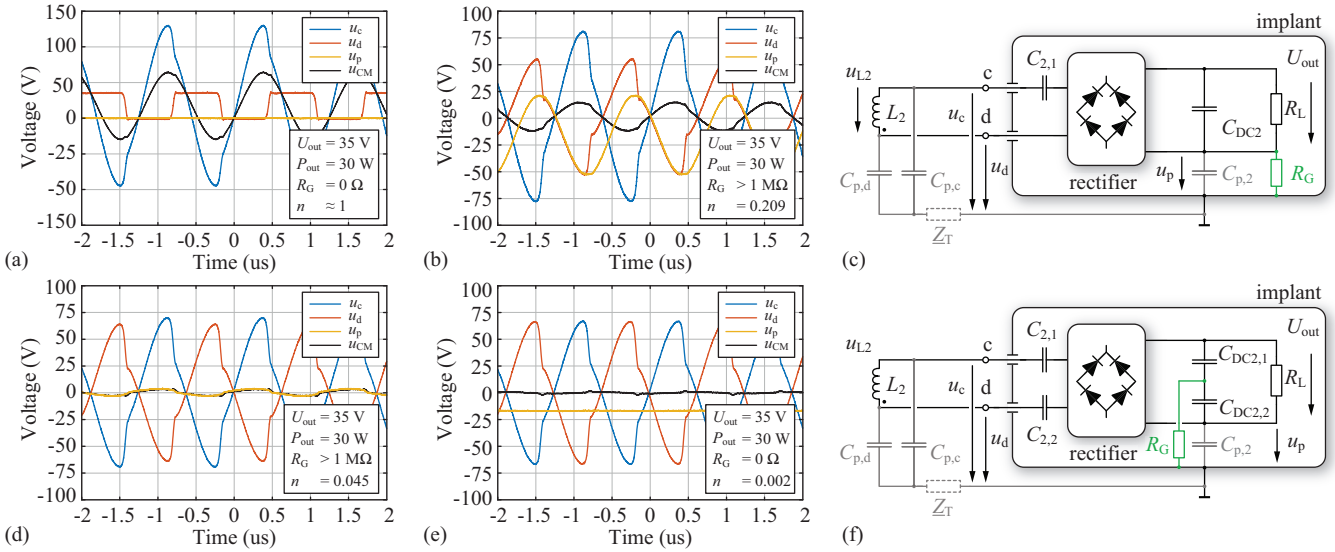

Figure 5: Results of the *in vitro* measurement of the receiver coil terminal voltages and calculated CM voltage with respect to the tissue surrounding the secondary side TET coil. (a) and (b) show the measured coil terminal voltages for the receiver topology shown in (c). (d) and (e) show the coil terminal voltages for the topology illustrated in (f).

voltage amplitude and the maximum SAR increases quadratically as expected from (1). The figures show that the impact of the CM voltage on the EMF exposure can be significant even with small CM voltage amplitudes. As indicated, the peak electric field strength can be reduced by increasing the thickness of the coil insulation layer. However, in order to enhance the implantabilty and the wearing comfort for the patient, the receiver coil should be designed as thin as mechanically and electrically possible.

Fig. 4(b) clearly shows that the considered power electronic topology with the CM-DM ratio of 0.05 to 0.45 is not a feasible solution for a high power TET system. Therefore, in the next section, four combinations of different grounding schemes and receiver topologies are compared in an *in vitro* experiment in order to identify a solution with a lower CM voltage.

C. In Vitro Experimental Validation

In order to validate the theoretical considerations of the previous section, an *in vitro* experiment was performed using a mock implant which includes a diode rectifier circuit, the resonant tank capacitors and an external resistive load. The implant was built such that a parasitic capacitance of 84 pF between the negative rail of the rectifier circuit and a ground plane is formed. The ground plane has a size of 25×38 mm and is electrically connected to the tissue. As a model for the human skin, a 200×200 mm piece of skin and subcutaneous tissue from the chest of a pig, including the pectoral muscle and ribs, was used. The receiver coil was inserted underneath the subcutaneous fat layer on top of the muscle in a distance of approximately 15 mm to the transmitter winding.

Two different topologies of the power electronic circuit with two different grounding schemes were considered. The first topology comprises a single secondary side resonant capacitor and either a low-resistance connection R_G or a capacitive coupling $C_{p,2}$ to the ground plane as indicated in **Fig. 5(c)**. The second topology uses a balancing of the power electronic circuit by means of the distribution of the secondary resonant capacitors between the input terminals of the rectifier circuit and either a low- or high-resistance ground connection R_G of the mid-point of the DC-link capacitors as indicated in **Fig. 5(f)**. The terminal voltages at the input of the receiver circuit and the voltage across the parasitic capacitance $C_{p,2}$ were measured with a LeCroy ADP305 differential voltage probe and the prototype TET system operated with an output power of 30 W and an output voltage of 35 V.

Fig. 5(a) shows the measured voltage waveforms for the receiver circuit shown in **Fig. 5(c)**, using a low-resistance connection R_G of the negative voltage rail of the rectifier to the ground plane. In this case, the full differential voltage of the secondary side coil is present at coil terminal c with respect to the surrounding tissue, causing a very high electric field strength in the tissue close to the edge of the TET coil. This can be regarded as a worst case scenario. **Fig. 5(b)** shows the measurement for the same resonant converter topology and for the case where the implant is only capacitively coupled to the surrounding tissue by the parasitic capacitance $C_{p,2}$. The CM-DM ratio is approximately 0.21 and is in good agreement with the estimated range of CM voltage. The previously discussed **Fig. 2** shows the simulation result of the magnitude of the electric field strength in the subcutaneous tissue for this specific operating point. It can be seen that specifically at the edge of the receiver coil, the amplitude of the electric field strength and also the SAR exceeds the basic restrictions proposed by the ICNIRP substantially.

Fig. 5(d) shows the measurement results for the second topology with the distributed resonant capacitors and a capacitive coupling $C_{p,2}$ of the circuit to the surrounding tissue. It can be seen, that the CM voltage is substantially reduced, but there is still an asymmetry between the coil terminal voltages. In order to further reduce the CM voltage, the mid-point of the DC-link capacitors $C_{DC2,1}$ and $C_{DC2,2}$ is connected to the ground plane of the mock implant directly ($R_G = 0\ \Omega$). In this case, as it is shown in **Fig. 5(e)**, the TET coil terminal voltages are fully symmetric and thus have the lowest voltage amplitude with respect to the tissue reference potential. However, in order to limit the contact current to a level well below the maximum permissible amount of 20 mA, as it is proposed as a reference level for general public exposure in ICNIRP 1998 [18], the DC-link mid-point can be connected to the enclosure of the implant using a resistive or inductive connection, with an impedance of 100-500 Ω. According to **Fig. 4(c)**, the peak SAR can be reduced from 2.3 W/kg to 1.21 W/kg using this topology and allows for compliance with the

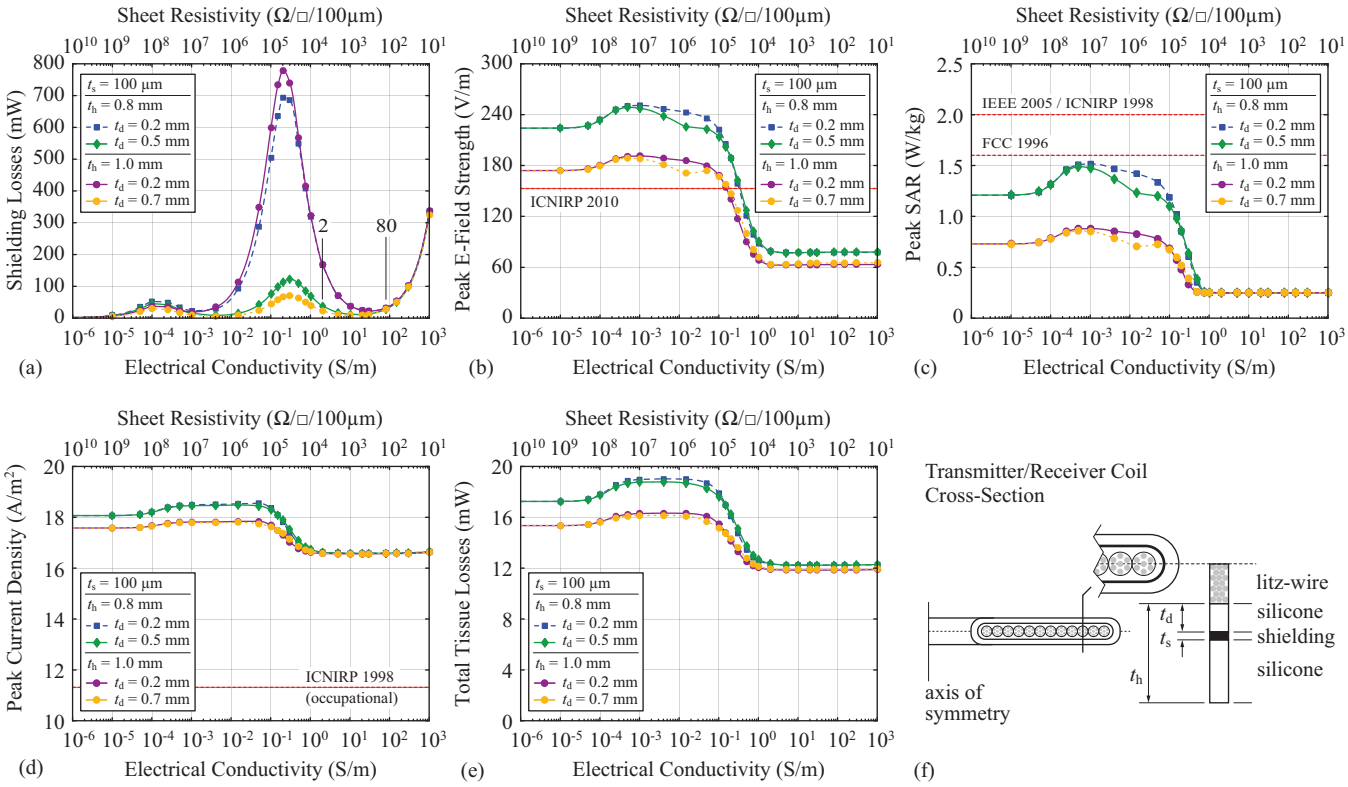

Figure 6: Simulation results of the power losses in the electric shielding (a), peak electric field strength in the tissue (b), peak SAR in the tissue (c), peak current density (d) and total power losses in the tissue (e), as a function of the electrical conductivity of the shielding material. (f) Schematic drawing of the cross-section of the energy transfer coils including the shielding layer.

basic restrictions. However, the peak internal electric field strength of 224 V/m still exceeds the basic restrictions significantly, if a coil insulation layer thickness of 0.8 mm is used. Therefore, an electric shielding of the TET coils is investigated in the following section in order to further reduce the peak electric field strength and the maximum SAR.

VI. Electric Shielding

It was shown in **Fig. 2** that the internal electric field has a maximum in close proximity to the receiver coil due to the comparably low electrical conductivity and permittivity of the fat tissue. The experiments in **Section V-C** have shown that even with a fully balanced power electronic circuit, the basic restriction on the internal electric field strength is exceeded. As a solution, the electric field strength can be reduced significantly if a layer of conductive material is used in addition to the electric insulation of the coils, which acts as an electric shielding.

In order to determine the optimal electrical conductivity of the shielding material, a parameter sweep was performed using the numerical simulation model presented in **Section IV**, where the electrical conductivity of the shielding material was varied from 10^{-6} S/m to 10^{3} S/m. The shielding layer encloses the entire receiver coil winding and is embedded within the silicone insulation as shown in **Fig. 6(f)**. The thickness of the shielding layer is 100 µm and the permittivity of the material is the same as for the silicone in order eliminate its influence on the simulation results. In addition, it was assumed that the proposed symmetric resonant converter structure and grounding scheme is used for the primary and secondary side of the TET system, such that no CM voltage applies to the TET coils. **Fig. 6(a)-(e)** show the simulation results for the total losses in the shielding material, the maximum internal electric field strength, the peak SAR, and the current density in the tissue as well as the total power losses in the tissue volume. The simulation was carried out for a coil insulation thickness of 0.8 mm and 1.0 mm and a variable distance of the shielding layer to the coil winding according to **Fig. 6(f)**. In **Fig. 6(a)** it can be seen that if the electrical conductivity of the shielding material is increased to about 0.01 S/m, the power losses in the shielding layer increase rapidly due to the increased mobility of charge carriers which are accelerated under the influence of the applied electric field. Due to the displacement of charge carriers, the applied electric field will be partly cancelled as the conductivity is increased and as a result, the losses in the shielding material start to decrease again. At this point, the magnitude of the electric field in the surrounding tissue decreases significantly as shown in **Fig. 6(b)**, since the shielding layer starts to form an equipotential surface around the coil windings. However, with increasing electrical conductivity, eddy currents are induced in the shielding layer due to the magnetic field and the shielding losses start to increase again. Hence, there is an optimal electrical conductivity of the shielding material in the range of 2-80 S/m, where the losses in the shielding layer are at a minimum and the peak electric field strength in the tissue is not decreasing any further. In this case, the shielding losses of 11 mW would contribute approximately 1 % to the total losses of 1.067 W measured with the prototype TET system operated at full output power and 15 mm coil separation distance. However, the shielding of the electric field in the vicinity of the receiver coil cannot protect from the induced electric field in the tissue caused by the alternating magnetic field. Therefore, the peak electric field strength, the peak SAR and the peak current density are not decreasing any further if the electrical conductivity of the shielding material is higher than about 1 S/m. The location in the tissue with the highest SAR value

is then not anymore at the edge of the receiver coil, but in the muscle tissue below the receiver coil, where the induced current density is the highest.

Materials with the desired electrical conductivity can be found in industry as carbon conductive composites, where a polymer is often used in combination with a conductive filler based on carbons in order to control the conductivity of the compound. As an example, conductive silicone rubbers are available in a large variety for electromagnetic shielding with a conductivity of 0.1 S/m to 100 S/m [24] and in a similar application, semiconductive tapes are used in the manufacturing of power distribution cables to provide a uniform electric field gradient to the dielectric insulation of the cable [25].

With the use of the described electric shielding method, the peak internal electric field strength was reduced by a factor of 2.9 to about 77 V/m and the peak SAR was reduced by a factor of 2.9 to 4.8 to about 0.25 W/kg, depending on the thickness of the silicone insulation layer. The achieved level of EMF exposure is, therefore, significantly lower than the basic restriction limits required by the exposure guidelines. However, the peak current density of 16.6 A/m^2 in the muscle tissue still exceeds the basic restriction limit substantially. The only possibility to decrease the current density is to use an additional shielding of the magnetic field below the receiver coil which will be a topic of future work.

VII. Conclusions

In this paper it was shown that the assessment of the EMF exposure on the human body based on the calculation of the induced electric field due to the time-varying magnetic field is not sufficient in the case of a TET system. The contribution of the electric field due to the high voltage at the receiver coil terminals can be significant, which it is specifically the case for a series-series compensation topology. Furthermore it was shown, that the magnitude of the internal electric field is highly dependent on the CM voltage at the receiver coil terminals and depends also on the power electronic topology of the implanted controller. In order to reduce the CM voltage and the EMF exposure to a minimum, the resonant tank of the TET system must be designed symmetrically and in addition, the midpoint of the DC-link capacitors of the implanted power controller must be connected to an enclosure which provides an electrical connection to the surrounding tissue. The internal electric field strength and the peak SAR can be further reduced with the use of an electric shielding layer around the energy transmission coils. For the prototype TET system at hand it was found that an electrical conductivity of the shielding material of 2-80 S/m is optimal which could be realized in practice using e.g. semiconductive tape or a carbon conductive compound as part of the TET coil's coating. Simulations have shown that the peak electric field strength and the peak SAR can be reduced from 224 V/m to 77 V/m and from 1.21 W/kg to 0.25 W/kg respectively, and comply with the EMF exposure guidelines.

Acknowledgment

The authors gratefully acknowledge the financial funding by the Baugarten foundation and would like to thank Hochschulmedizin Zürich for the support in this project.

References

[1] J. C. Schuder, "Powering an artificial heart: birth of the inductively coupled-radio frequency system in 1960," *Artif. Organs*, vol. 26, no. 11, pp. 909–915, 2002.

[2] C. A. Milano and A. A. Simeone, "Mechanical circulatory support: devices, outcomes and complications," *Heart Failure Reviews, Springer US*, vol. 18, no. 1, pp. 35–53, 2010.

[3] S. Maniar, S. Kondareddy, and V. K. Topkara, "Left ventricular assist device-related infections: past, present and future," *Expert Rev. Med. Devices*, vol. 8, no. 5, pp. 627–634, 2011.

[4] D. Pereda and J. V. Conte, "Left ventricular assist device driveline infections." *J. Cardiol. Clin.*, vol. 29, no. 4, pp. 515–527, 2011.

[5] M. S. Slaughter and T. J. Myers, "Transcutaneous energy transmission for mechanical circulatory support systems: history, current status, and future prospects," *J. Card. Surg.*, vol. 25, no. 4, pp. 484–489, 2010.

[6] T. D. Dissanayake, "An effective transcutaneous energy transfer (TET) system for artificial hearts," Ph.D. dissertation, Inst. Bioeng., Univ. Auckland, Auckland, New Zealand, 2010.

[7] O. Knecht, R. Bosshard, J. W. Kolar, and C. T. Starck, "Optimization of transcutaneous energy transfer coils for high power medical applications," in *Proc. IEEE Control Modeling Power Electron. Conf. Expo.*, 2014, pp. 1–10.

[8] A. Christ, M. Douglas, J. Nadakuduti, and N. Kuster, "Assessing human exposure to electromagnetic fields from wireless power transmission systems," *Proc. IEEE*, vol. 101, no. 6, pp. 1482–1493, 2013.

[9] I. Laasko, T. Shimamoto, A. Hirata, and M. Feliziani, "Applicability of quasistatic approximation for exposure assessment of wireless power transfer," in *Proc. IEEE Int. Symp. Electromagn. Compat.(Tokyo))*, 2014, pp. 430–433.

[10] X. L. Chen, A. E. Umenei, D. W. Baarman, N. Chavannes, V. De Santis, J. R. Mosig, and N. Kuster, "Human exposure to close-range resonant wireless power transfer systems as a function of design parameters," *IEEE Trans. Electromagn. Compat.*, vol. 56, no. 5, pp. 1027–1034, 2014.

[11] T. Sunohara, A. Hirata, I. Laakso, and T. Onishi, "Analysis of in situ electric field and specific absorption rate in human models for wireless power transfer system with induction coupling," *Phys. Med. Biol.*, vol. 59, no. 14, pp. 3721–3735, 2014.

[12] K. Shiba and N. Higaki, "Analysis of SAR and current density in human tissue surrounding an energy transmitting coil for a wireless capsule endoscope," in *Proc. 20th Int. Zurich Symp. EMC*, 2009, pp. 321–324.

[13] L. Lucke and V. Bluvshtein, "Safety considerations for wireless delivery of continuous power to implanted medical devices," in *Proc. IEEE Int. Conf. Eng. Med. Biol. Soc. (EMBC)*, 2014, pp. 286–289.

[14] K. Shiba, M. Nukaya, T. Tsuji, and K. Koshiji, "Analysis of current density and specific absorption rate in biological tissue surrounding transcutaneous transformer for an artificial heart," *IEEE Trans. Biomed. Eng.*, vol. 55, no. 1, pp. 205–213, 2008.

[15] O. Knecht, R. Bosshard, and J. W. Kolar, "High-efficiency transcutaneous energy transfer for implantable mechanical heart support systems," *IEEE Trans. Power Electron.*, vol. 30, no. 11, pp. 6221–6236, 2015.

[16] *Guidelines for evaluating the environmental effects of radiofrequency radiation*. Federal Communications Commission, FCC 96-326, Washington, D.C., USA, 1996.

[17] *IEEE standard for safety levels with respect to human exposure to radio frequency electromagnetic fields, 3 kHz to 300 GHz*. IEEE International Commitee on Electromagnetic Safety, IEEE C95.1-2005, IEEE, New York, NY, USA, 2005.

[18] ICNIRP, "*Guidelines for limiting exposure to time-varying electric, magnetic and electromagnetic fields (up to 300 GHz)*," *Health Phys.*, vol. 74, no. 4, pp. 494–522, 1998.

[19] ——, "*Guidelines for limiting exposure to time-varying electric and magnetic fields (1 Hz - 100 kHz)*," *Health Phys.*, vol. 99, no. 6, pp. 818–836, 2010.

[20] The IT'IS Foundation Website (2015, Apr.), "Database of tissue properties." [Online]. Available: http://www.itis.ethz.ch/virtual-population/tissue-properties/database/

[21] C. Gabriel, *Compilation of the dielectric properties of body tissues at RF and microwave frequencies*. Report N.AL/OE-TR- 1996-0037. Occupational and environmental health directorate, Radiofrequency Radiation Division, Brooks Air Force Base, Texas (USA), 1996.

[22] J. Larsson, "Electromagnetics from a quasistatic perspective," *Am. J. Phys.*, vol. 75, no. 3, pp. 230–239, 2007.

[23] N. Orcutt and O. P. Gandhi, "A 3-D impedance method to calculate power deposition in biological bodies subjected to time varying magnetic fields," *IEEE Trans. Biomed. Eng.*, vol. 35, no. 8, pp. 577–583, 1988.

[24] Shin-Etsu Silicone Global (2015, May), "Electrically conductive silicone rubber products." [Online]. Available: http://www.shinetsusilicone-global.com/catalog/pdf/ec_e.pdf

[25] S. J. Han, A. Mendelsohn, and R. Ramachandran, "Overview of semiconductive shield technology in power distribution cables," in *Proc. IEEE PES Transmission and Distribution Conf. and Exhibition*, 2006, pp. 641–646.